JOURNAL OF MATERIALS SCIENCE **40** (2005) 6241–6248

Mechanical properties and damage evaluation of a UK PBX

K. ELLIS, C. LEPPARD, H. RADESK
AWE Plc,Aldermaston, Reading, Berkshire, RG7 4PR

Published online: 8 September 2005

This study outlines the mechanical properties of an explosive material tested at AWE Plc, Aldermaston, Reading, Berkshire, UK. The material is a composite polymer bonded explosive of energetic binder and HMX crystals, referred to as EDC37. An understanding of material deformation under a range of conditions and age, along with damage quantification, is required to predict mechanical behaviour throughout service life. The mechanical testing of EDC37 was performed alongside simultaneous recording of Acoustic Emission (AE) data at static strain rates and temperatures. The simultaneous testing was intended to focus on the link between mechanical properties and damage evolution. Forty tests were performed in various configurations, consisting of live explosive material and an inert simulant. Evaluation of the Acoustic Emissions was performed and data grouped into categories of activity. It was concluded that AE confirms mechanical behaviour associated with damage accumulation in compression (crack initiation and growth, crack closure and/or HMX twinning) and crack damage (binder HMX debonding and coalescence) above a threshold stress or time in tension. The activity seen is different between tensile and compressive modes and needs to be taken into consideration in Finite Element Models.

1. Introduction

The mechanical properties of explosive materials, subject to a range of conditions with age, are important criteria for determining a safe working life. This work aims to investigate the link between mechanical properties and damage evolution by simultaneously recording acoustic emissions during compressive, tensile and flexure testing at static strain rates (10^{-5} s^{-1}) and room temperature. The results endeavour to provide insight into the dominant failure modes of the explosive for finite element (FE) model development and prove Acoustic Emission (AE) technology as a diagnostic tool.

The Polymer Bonded Explosive (PBX) formulation used in this study, EDC37, is formed from 9% w/w nitrocellulose based gelatinous binder and 91% w/w crystalline HMX. The particle size of beta-HMX has been measured by laser light scattering techniques giving a D(4,3) value of 44.7 microns, where all particles pass through a 125 micron sieve [1]. The viscous binder is amorphous with a glass transition[1] temperature lower than ambient. The composite comprises of a high percentage of HMX covered by the viscous binder with a small degree of porosity (measured densities for EDC37 approach the theoretical maximum density for the solid).

The failure of all engineering materials, including PBXs, can be described as either ductile or brittle [3] and classification is based on the ability of a material to experience plastic deformation. Ductile materials typically exhibit substantial plastic deformation with high energy absorption before fracture, and with brittle failure little or no plastic deformation and low energy absorption. Typically materials show a transition from brittle to ductile with temperature or strain rate. At the proposed static strain rate and moderate temperature considered for EDC37, it is expected that failure will lie between the described brittle or ductile behaviour and may also depend on the mode of stress application. Both ductile and brittle failures involve the process of crack generation and quantifying the amount of crack damage in EDC37 is the ultimate goal for FE model development.

One way of measuring damage is through acoustic emission during mechanical testing [4, 5]. Structural or microstructural alteration in the solid material, considered as mechanically induced damage, generates a transient elastic wave by the rapid release of strain energy. At the binder-HMX interface, or within the HMX

[1]Glass Transition Temperature of Nitrocellulose/Binder is approximately –60°C [2].

0022-2461
DOI: 10.1007/s10853-005-3148-4

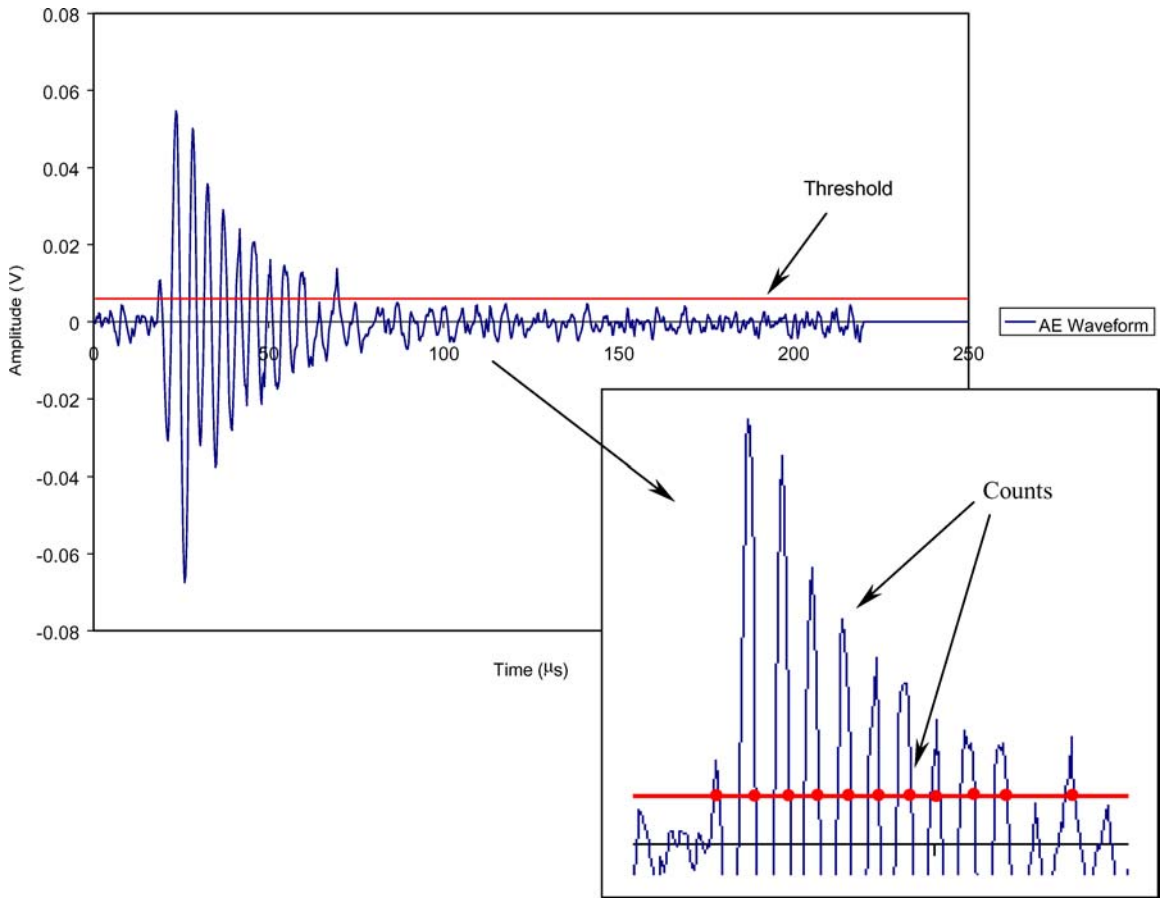

Figure 1 Typical transient elastic wave produced during a test. The horizontal line indicates the threshold and the number of counts associated with this single hit is shown in the enlarged part of the figure.

itself, the possible causes of damage processes include debonding, crack initiation and growth and crack closure. Dislocation movement and mechanical twinning are to be considered for the HMX crystals alone. However for the binder, any mechanically induced crack tip will have a very low stress intensity energy associated with it and crack blunting through binder flow will dominate in preference to crack propagation.

Each acoustic detection is called a 'Hit' or 'Event' and produces a single waveform in the data set. This waveform has a number of 'Counts' associated with it, (see Fig. 1); this count value demonstrates the amount of AE that is occurring and to some extent the severity of an 'event'. The Hit and Count data are used in the first instance to establish the amount of activity occurring and the feasibility of the elastic wave generating-damage processes when considering EDC37. Further quantification of all data are then considered, for example, removing unwanted measurements and counting the number of elastic events which indicate internal structure change (or damage) for each individual mechanical test. This paper is thus a first stage assessment of the amount of damage contribution to the stress-strain curve of EDC37 in tension, 3-point bend and compression.

2. Method

Mechanical testing of EDC37 was carried out at AWE, Aldermaston, Reading. Owing to the nature and mass of the material involved all mechanical tests are carried out under isolated conditions using a specially adapted Instron test machine 5500R1185.

In compression a uniaxial stress was applied to the cylindrical specimen using a compression cage. The cage is a rigid structure ensuring parallel platen compression to the ends of the specimens. Above and below the cage, out of alignment issues were dealt with by the use of rose joints/ball fixings. Strain was measured directly on the specimen by two knife-edge extensometers situated opposite one another around the specimen circumference. All tests were carried out in a thermal cabinet capable of maintaining temperatures from –20°C to 80°C to ±1°C. Each compression specimen measures nominally 50 mm high by 20 mm diameter.

In tension, explosive specimens were supplied as cylindrical dumbbell geometries measuring 80 mm high by 10 mm diameter. These specimens were bonded into polythene end caps using a compatible adhesive. Rig misalignment was reduced by the use of ball joints above and below the specimen and a single knife-edge extensometer was then attached to the specimen to measure strain.

In flexure rectangular bars were made to geometry 12 mm square by 114 mm. They were placed into an in-house designed rig which allows movement in two-dimensions to accommodate non-parallelism in the opposite faces of the rectangular specimen. Load was applied to the specimen at its centre position, over a span of 102 mm, and displacement measured via an

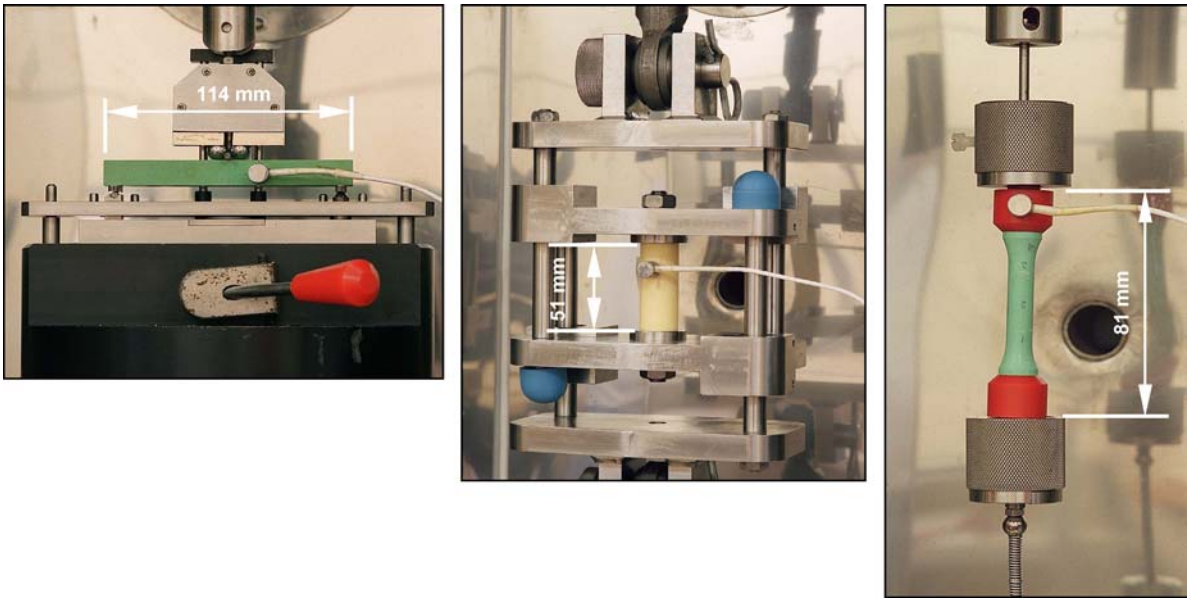

Figure 2 Photographs of test configurations in flexure, compression and tension including transducer locations.

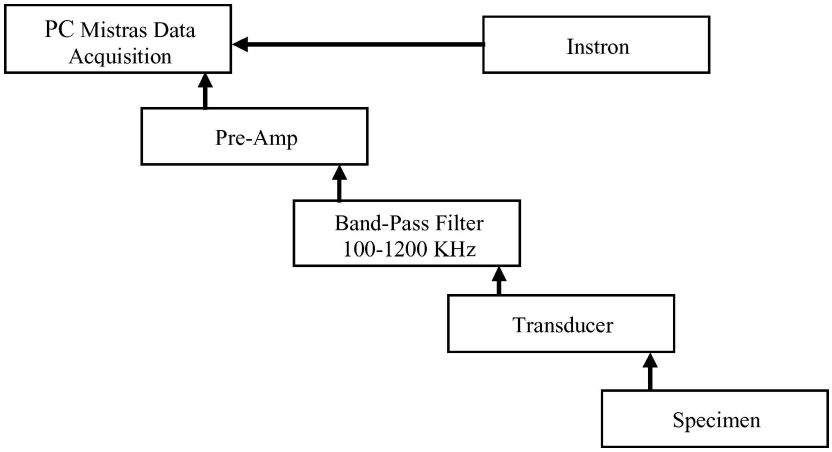

Figure 3 Systematic flow diagram of apparatus used to conduct experiments.

extensometer situated at the rear, adjacent to the specimen (which measures the centre displacement of the bar during the flexure test).

Specimens were sourced from 2 charge pressings, that is from a single source of PBX powder pressed at different stages. This separation was made as sometimes mechanical properties can vary across charges. Examples of specimens housed in the compression, tensile and flexure rigs are given in Fig. 2. This figure does not show the extensometers.

Mechanical testing was carried out at a speed of 0.2 mm/min in each case and the temperature was controlled at 20°C. The rate of testing in compression was an average of 40 $\mu\varepsilon s^{-1}$. Flexure and tensile tests were conducted at an average rate of 23 $\mu\varepsilon s^{-1}$.

The AE equipment utilised was the Mistras 2001 system from Physical Acoustic Corporation (version E2.23). The system included preamplifiers with variable gain and band pass filters allowing data collection between 100–1200 kHz. Transducers were also from PAC, and are Micro 30 Ds operating over 100–600 kHz range. The transducer output voltage was amplified and filtered before being processed by the data acquisition equipment. A schematic system diagram for the set-up can be seen in Fig. 3. Piezoelectric transducers were coupled to specimens using a silicon-based material known as Sylgard 184. Locations were chosen to minimise effects from the apparatus and to ensure maximum data acquisition (proximity to likely crack locations). For the dumbbell, it was not possible to locate transducers on the gauge length however initial evaluation showed that the use of end-cap located transducers provided acceptable data, with sufficient correlation between all transducer locations. Fig. 4 shows the locations on tensile dumbbells.

In the first instance non-explosive flexure beams (inerts) were tested to perfect the settings for preamplification and threshold before commencing with explosive test specimens. The inert was formulated from a melamine particulate filler with a similar binder and was not considered a representative mechanical property simulant. Values of 60 db pre-amplification and a floating lower limit were chosen (to guarantee events above background noise were recorded). A baseline between the two acquisition systems (the AE and Instron) was ensured by the AE system logging the same load output from the Instron.

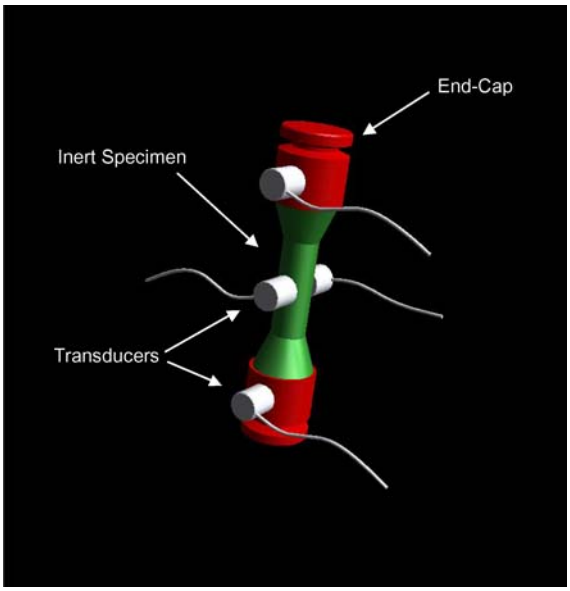

Figure 4 Transducer locations on tensile test dumbbell. Used to select most appropriate position for transducers during subsequent tests.

3. Results and discussion

Fig. 5 shows typical stress-strain plots of 16 specimens tested in each of the given test modes without interference from AE transducers. It is clear that the material exhibits higher compressive failure strengths than flexure, which are in turn greater than the ultimate tensile strengths at this strain rate and temperature. See Fig. 6 for a direct comparison of maximum/failure strengths. The data from the two charges show good read across and were subsequently considered as a single family.

In compression EDC37 demonstrates little extended linear elastic behaviour with no obvious yield point. Most of the stress-strain plot shows a curve with reducing slope towards failure as damage to the specimen progresses during the test. A great amount of plastic deformation is apparent and the area underneath the curve (indicating the energy required to cause fracture) is greatest under compression. Under this test mode EDC37 demonstrates ductile behaviour [6]. By contrast EDC37 demonstrates brittle behaviour under tension, and to a lesser extent in flexure, showing little or no plastic deformation prior to failure. There is also increased scatter in the ultimate stresses at failure under tension than under compression.

Visual observations of samples tested past the point of failure (up to typically 1.1 to 1.2% strain) show extensive surface cracking in compression (see Fig. 7). Numerous cracks are visible at 45° to the stress axis in a cross-hatching form suggesting shear failure. In tension samples break typically within the gauge length via what appears to be a single flaw. In flexure, samples crack apart at a point directly underneath the point of loading with no other visible cracks along the sample length.

The relatively lower tensile failure strength and increased scatter in the failure data give a first indication of the sensitivity of the PBX to flaws and cracks in tension. The spread in tensile data reflects the differences in flaw population characteristics from specimen to specimen inherent before tensile testing [6]. In contrast, the PBX still retains strength after extensive plastic deformation and visibly displays multiple cracking following compression. The failure of the PBX appears to be less sensitive to the number and accumulation of visual microcracks under compressive forces.

AE tests were performed with the inert as a first step that ensured a suitable process of measurement can be applied to an explosive material, with meaningful results reported. Approximately 40 AE-mechanical tests were performed, consisting of equal amounts of both inert and PBX specimens. PBX specimens produced good AE with flexure beams showing a few events during the test but most data acquired imminently

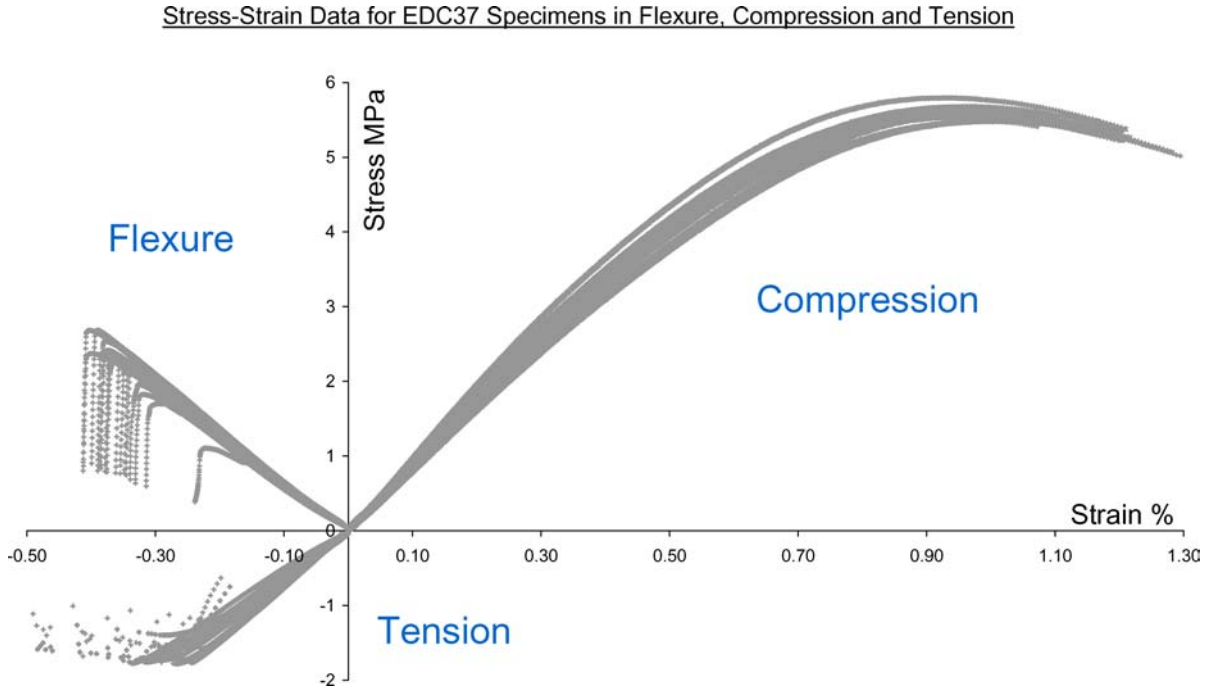

Figure 5 Stress-strain plots of EDC37 samples in compression, tension and flexure at constant test speed.

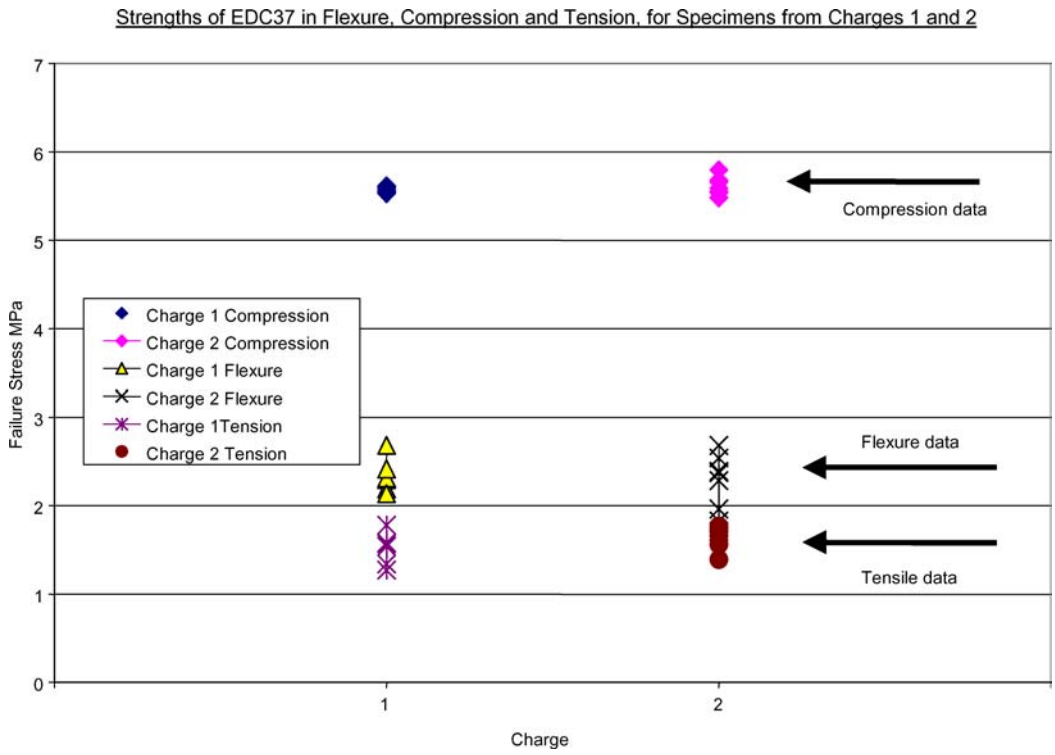

Figure 6 Failure stresses of EDC37 specimens from Charges 1 and 2 for compression, tension and flexure, without AE monitoring. This was used as a baseline to compare AE results.

before failure. Similar results were obtained for tensile specimens, which produced the least amount of data and most of it occurring just before mechanical failure. Under compressive forces a medium to large number of events were recorded for the PBX and were fairly spread-out through the test from the start of the test to failure. Fig. 8 shows examples of stress-strain plots and simultaneous AE data in flexure, compression and tension for EDC37.

The acoustic data was further evaluated where it was shown that not all activity was associated with elastic events; for example, emission from the mechanical testing apparatus, noise and unclear acoustic emissions were detected as well. All three tests modes included unwanted events and hence strengthened the need to evaluate waveforms. In order to provide this quantification resulting waveforms were split into categories, (i) elastic events (ii) multiple events (iii) noise (iv) abnormal waveforms and (v) unclear. Fig. 9 shows the types of waveforms mentioned. Furthermore, emission from the apparatus was measured and subtracted from the elastic events data set. This separation enabled elastic events emanating from the specimens to be related directly to stress-strain data.

The results demonstrate that only a few acoustic elastic events are detected in tensile test modes (both pure tension and flexure) near the point of failure (the examples in Fig. 8 show 7 occurrences of elastic events in tension and 155 in flexure, respectively), whereas under compression a large amount of activity was apparent throughout the test. In compression 368 events are shown in Fig. 8. A threshold limit is not evident (for example a limit of stress or strain above which an AE is heard) under compression as events take place from the very start of testing. However in tensile and flexure the first definite elastic events only occur after a high percentage of failure stress is reached (70–90% typically). This together with a more linear stress-strain response in tension shows that cracking requires a time or stress level to be reached before crack damage to failure initiates. This observation appears consistent with others [7] which note that the linear elastic region is associated with an incubation stage of acoustic activity.

The larger number of elastic events detected in compression, compared to that measured in flexure and tension, could simply be related to the volume fraction of material subjected to stress. For example, compression cylinders are the greatest in volume of all the test pieces and if it were true that only one damage process was operating the greatest number would be detected in compression. Counting the elastic wave data however discounts the simple relationship to volume. The gauge volume in tension is approximately half that considered for flexure and is a seventh of that experienced in compression. The number of elastic wave occurrences, however, do not follow the simple volume-scaling trend so different damage processes must occur in compression and tensile test modes.

The small number of elastic events in tension, just prior to fracture and the brittle stress-strain behaviour of the material together suggest that these specimens lead rapidly to failure by what appears to be a single (or low number of) crack(s). The microscopic mechanisms for crack initiation and propagation in tension for EDC37 have been investigated by other authors [8]. Their study at static rates suggests that predominant failure in tension starts at the edges of larger filler particles and separation occurs between the particles and binder. These link up and continue to extend and open, resulting in predominantly transgranular

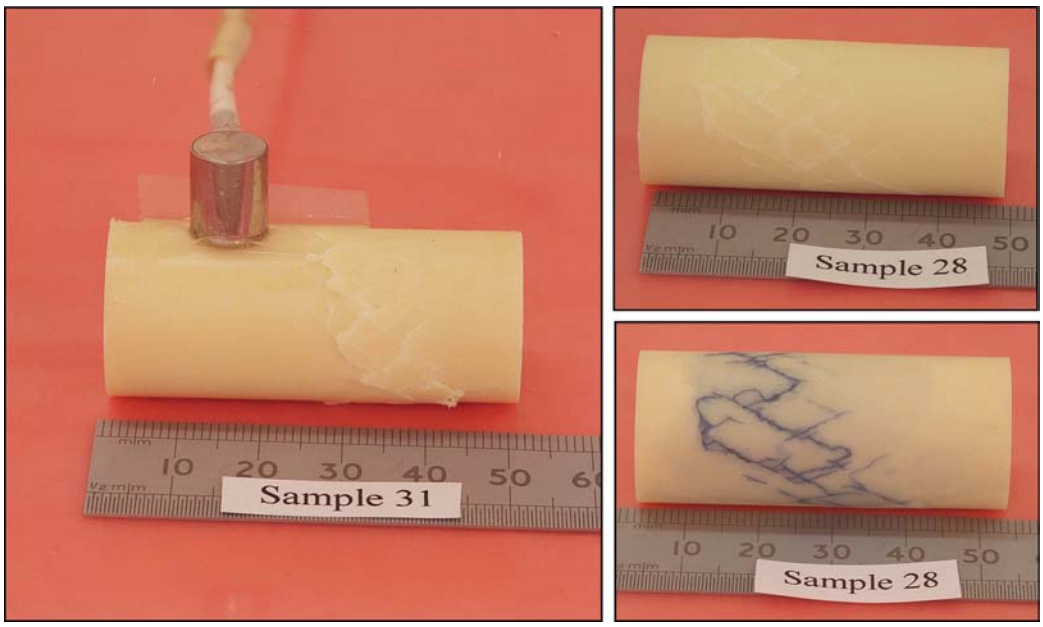

Figure 7 Physical test specimen showing extensive cross-hatching of EDC37 in compression, post test.

failure. Hence in the tensile mode of test, binder separation from the HMX, leading to crack initiation and rapid fracture is the likely explanation for the acoustic emission.

By contrast, in compression, the large number of acoustic events occurring throughout the tests infers that damage (possibly crack initiation, crack closure and/or HMX twinning) occurs from the very onset of applied stress. Indeed these events may happen in differing degrees at given levels of stress, with overlap, up to the maxima in the stress-strain curve. The larger number of acoustic events appear consistent with a non-linear stress-strain curve indicating damage. Further work should focus on identifying methods that can separate out the contribution from each damage mechanism and relate them to the stress-strain curve, currently this has not been performed on EDC37. It is possible however to suppose which damage mechanism occurs over a range of stresses. At low applied compressive stresses, non-linear stress-strain behaviour coupled

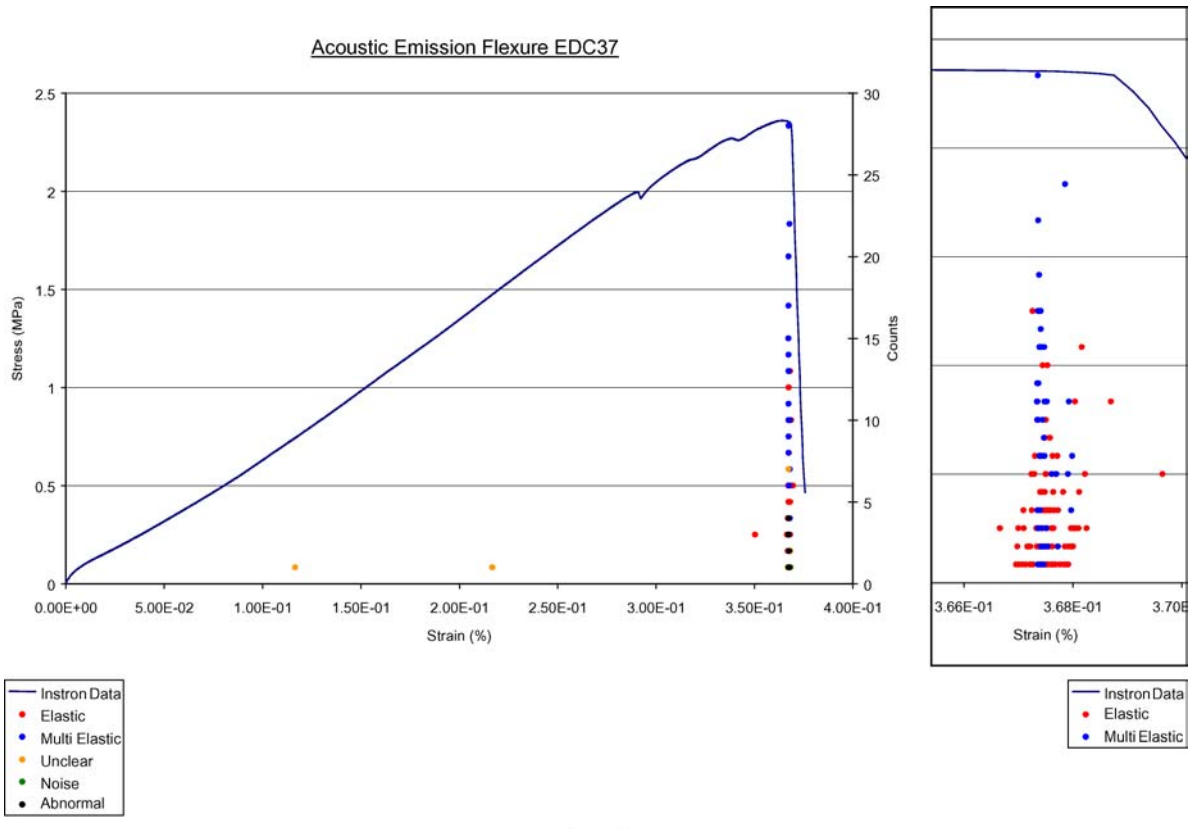

Part - 1

Figure 8 Flexure, compression and tensile stress-strain graphs with simultaneous AE data plotted. *(Continued.)*

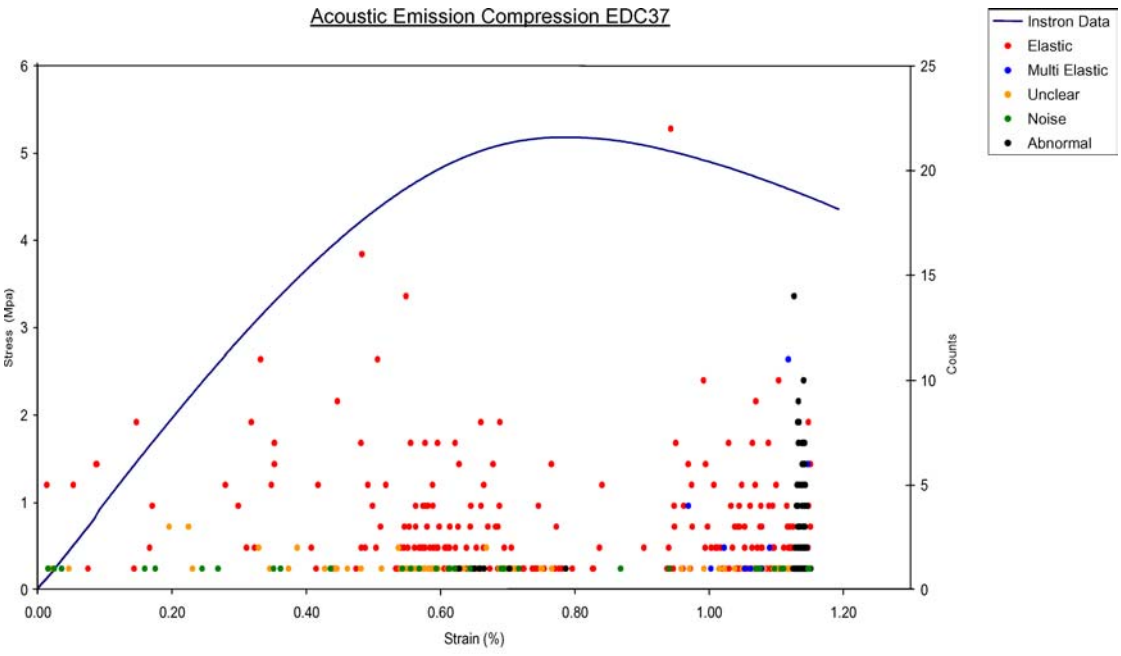

Part - 2

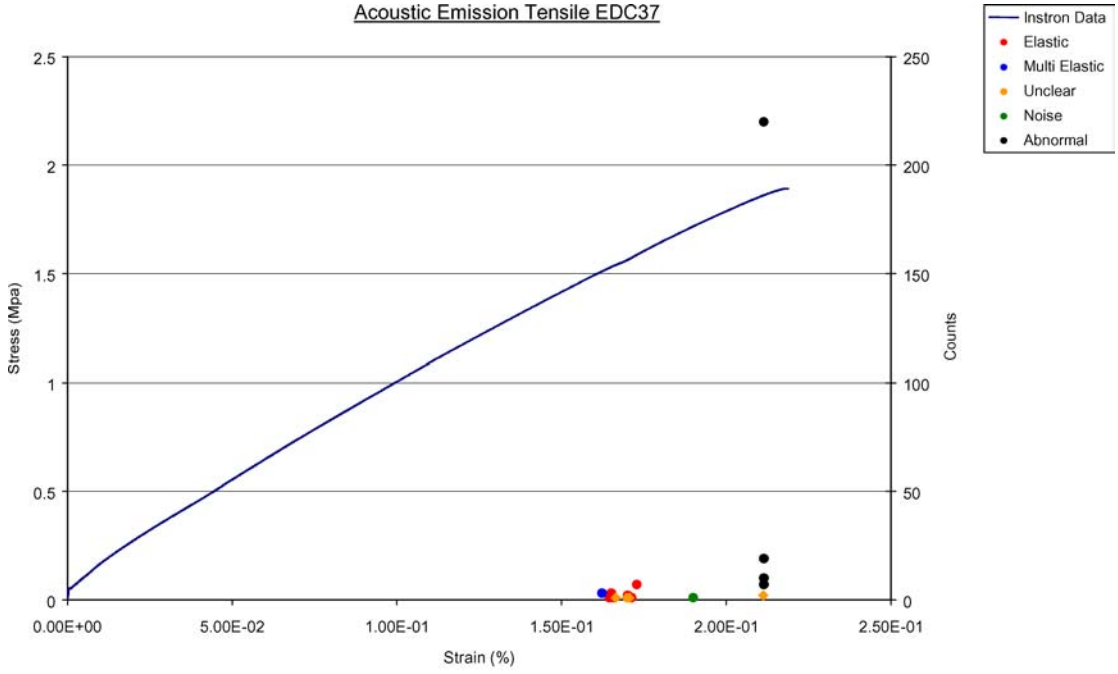

Part - 3

Figure 8 (Continued.)

with AE suggests low energy processes are operating. For example, HMX-binder crack and debonding closure/opening. Mechanical twinning in HMX is an elastic reversible process but can be permanent if local threshold stresses are exceeded. Some researchers have noted permanent mechanical twins in EDC37 tested under light to moderate applied stresses [9] evident by microstructural examination. Lastly, crack propagation and HMX dislocation activity are likely to occur at stresses near to that of fracture. The ductile nature in compression, showing higher energy absorption than in tension or flexure, and a greater number of acoustic elastic events suggests a reduced sensitivity of the maximum stress (failure stress) to damage in this test mode.

For the flexure specimen, below the neutral stress axis the material is in the tensile test mode and above this the material is in compression. It is no surprise therefore that the failure stress/strain for these specimens and the corresponding acoustic data lies between the data for compression and tension. In flexure, the failure appears similarly crack dominated. A smaller contribution of AE occurs in flexure, than that in compression, indicating some damage accumulation leading up to fracture.

The failure of EDC37 thus shows sensitivity to cracks under tensile stresses and a reduced sensitivity to cracks and other damage processes under compression. This means that crack damage, mechanical twinning or HMX dislocation contribute to the plastic strain and slope decrease which lead to slow crack failure under compression. Under tensile stresses it seems likely that cracking does not contribute to the majority of the

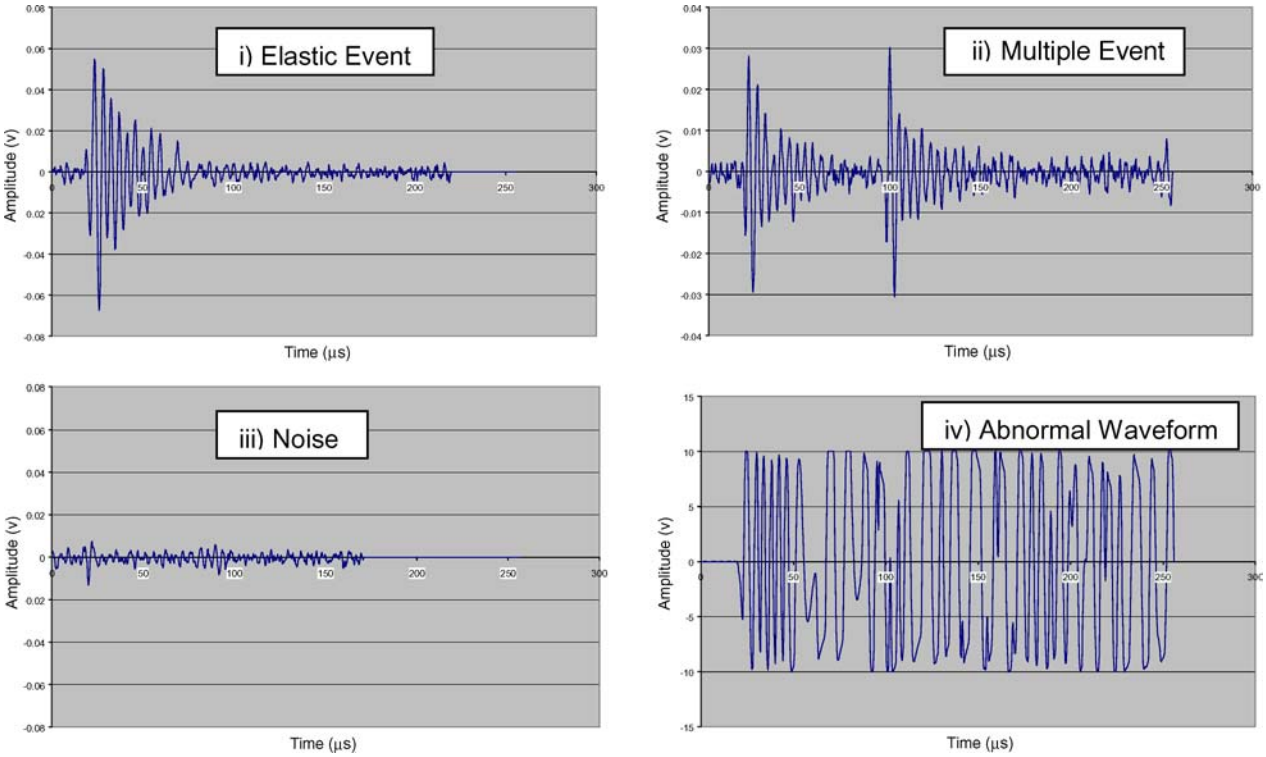

Figure 9 Example of categories of waveform observed from acoustic emission data produced in the compressive specimen test shown in Fig. 8 — Part 2. The four main waveforms seen here are elastic events, multiple elastic events, noise and abnormal.

stress-strain curve but is highly significant near to and just at failure. FEA models thus need to reflect brittle crack sensitive failure under tensile forces and slower ductile damage accumulation up to failure under compression. Other researchers using AE in flexure alone have shown comparable success of the AE technique to identify crack damage [10] in their PBXs.

4. Conclusion

Acoustic emission has proven to be a useful diagnostic to link damage accumulation processes to the mechanical behaviour of a UK PBX in tension, flexure and compression. EDC37 demonstrates ductile behaviour under compressive stress with little extended initial linear stress-strain behaviour. A large amount of plastic strain and a continuously reducing stress-strain slope is evident through damage accumulation (crack damage, HMX twinning and/or HMX dislocation). Under tensile stresses, cracking does not contribute to the majority of tensile strain demonstrated by an absence of AE. A time or stress level (found to be typically 70–90% of failure stress) threshold seems evident before cracking to failure occurs.

In all cases waveform data analysis is required to exclude unwanted events from the complete data set, this allows those events relating to damage to be evaluated (elastic wave generated). Exact quantification of the damage processes cannot be carried out by AE and investigation into alternative techniques is recommended for future work.

Finite element models need to reflect brittle crack sensitive failure under tensile forces and ductile damage accumulation up to failure under compression to correctly describe the mechanical damage mechanisms of EDC37.

Acknowledgements

Acknowledgements and thanks to Mr Paul Blackwell, Mr Paul Tatum and Mr Kevin Dalby, AWE Aldermaston, for their assistance in mechanical testing and acoustic emission guidance.

References

1. P. BOLTON *et al.* "A comparative study of techniques for the determination of particle properties of crystalline explosives, Energetic Materials Structure and Properties," in 35th International Annual Conference of ICT, June 29–July2, 2004, pp. 65-1–65–13.
2. R. GOVIER, The study of Thermally Induced Phase Transitions in a Nitrocellulose and K 10 Polymer Binder System, Degree Thesis, Brunel University and Trowbridge College, April 2000.
3. W. D. CALLISTER, "Materials Science and Engineering an Introduction," 6th edn. (Wiley International Edition, 2003).
4. A. G. BEATTIE, "Acoustic emission, principles and instrumentation," *J Acoust Emiss*, vol. 2, nos. 1/2, Acoust Emiss, Group, 1983.
5. J. R. MATTHEWS, "Acoustic Emission—NDT Monographs and Tracts", (Gordon & Breach Science Publishers Inc., New York, 1983).
6. J. C. ANDERSON *et al.* "Materials Science", 4th edn. (Stanley Thornes Publishers Ltd, 1998) p. 311.
7. FANG and BERKOVITS, *Trans. ASME*, **117** (1993) 200.
8. P. RAE *et al.*, *Proc. of Royal Society* **458** (2002) 2019, 743–762.
9. PRIVATE COMMUNICATION, S. PALMER, "Cavendish Laboratory", (Cambridge University, England).
10. L. JINGRUN *et al.* Monitoring the Damage Evolution of PBX by Acoustic Emission, Proc. of the 4th International Autumn Seminar on Propellants, Explosives and Pyrotechnics, 2001.

Received 22 December 2003
and accepted 9 May 2005